A Two-stage Stochastic Model for Coordinated Operation of Natural Gas and Microgrid Networks

Author(s): Zandrazavi, Seyed Farhad; Tabares, Alejandra; Franco, John Fredy; Shafie-Khah, Miadreza; Soares, João; Vale, Zita

Title: A Two-stage Stochastic Model for Coordinated Operation of Natural Gas and Microgrid Networks

Year: 2023

Version: Accepted manuscript

Please cite the original version:

Zandrazavi, S. F., Tabares, A., Franco, J. F., Shafie-Khah, M., Soares, J. & Vale, Z. (2023). A Two-stage Stochastic Model for Coordinated Operation of Natural Gas and Microgrid Networks. In *2023 IEEE Belgrade PowerTech*. IEEE. https://doi.org/10.1109/PowerTech55446.2023.10202794

A Two-stage Stochastic Model for Coordinated Operation of Natural Gas and Microgrid Networks

Seyed Farhad Zandrazavi
Department of Electrical Engineering
São Paulo State University
Ilha Solteira, Brazil
sf.zandrazavi@unesp.br

Alejandra Tabares
Department of Industrial Engineering
Los Andes University
Bogotá, Colombia
a.tabaresp@uniandes.edu.co

John Fredy Franco
Department of Electrical Engineering
São Paulo State University
Ilha Solteira, Brazil
j.f.franco@ieee.org

Miadreza Shafie-khah
School of Technology and Innovations
University of Vaasa
Vaasa, Finland
mshafiek@uwasa.fi

João Soares
GECAD, School of Engineering (ISEP)
Polytechnic of Porto
Porto, Portugal
jan@isep.ipp.pt

Zita Vale
GECAD, School of Engineering (ISEP)
Polytechnic of Porto
Porto, Portugal
zav@isep.ipp.pt

***Abstract*— On the one hand, natural gas-fired dispatchable distributed generation (DG) units and batteries can be used in microgrids (MG) to cope with the intermittency of renewable energy resources such as wind turbines and photovoltaic units. On the other hand, the uncertainties in MG influence the gas system through the gas-fired DG units, making these systems' optimal operation interdependent. As a result, firstly, a novel mixed-integer nonlinear model for optimal integrated operation of gas and MG networks is proposed. Then, the model is linearized, guaranteeing the optimality of solutions and enhancing the model's tractability. Finally, a two-stage stochastic mode is proposed to include the uncertainties linked to electricity price, wind power speed, solar irradiation, and demand. In contrast, the value of the stochastic solution measurement is calculated to justify the use of the stochastic approach. The results indicate that the total cost of the integrated system decreased by 17.82% using the stochastic model compared to the deterministic approach.**

Keywords—energy management, gas distribution network, microgrid, renewable energy, stochastic programming

I. INTRODUCTION

Climate change and its damaging consequences are threatening the future of humankind on Earth. As a result, to mitigate greenhouse gas (GHG) emissions, the European Commission aimed to reach net zero GHG emissions and a climate-neutral state by 2050. Furthermore, at the global level, the Paris Agreement was signed by 194 members of the United Nations Framework Convention on Climate Change in 2015, endeavoring to restrict global warming below 1.5◦C [1]. Therefore, the sustainable development of renewable energy resources is critical to reducing GHG emissions and accomplishing these stated objectives [1]. Microgrids (MGs) are considered an efficacious solution for renewable energy transition and GHG reduction by providing infrastructures for the integration of renewable energy-based distributed generation (DG) units such as wind turbines and photovoltaic units as well as electric vehicle charging stations [2]. However, renewable-based DG units' power generation is inherently intermittent and uncertain because of renewable energy dependence on weather conditions. Integrated electricity-gas distribution networks are proposed in the literature since the integrated network indicates more operational flexibility than the separated ones [3] to moderate the adverse effects of renewable generation uncertainty. In addition, according to previous studies, integrating gas and electricity networks can enhance the resiliency of the systems against extreme events [4], [5]. Uncertainties play decisive roles in the optimal operation of MGs as the optimality and feasibility of the solutions depend on the value of forecasted parameters. Scenario-based stochastic programming is deployed in this study to address uncertainties linked to wind speed, solar irradiation, and energy demand. Due to its effectiveness and applicability, stochastic optimization has been used widely to address uncertainties in the integrated gas and electricity networks in the literature [6]. However, quality matrices such as the value of the stochastic solution (VSS) [7] are not considered in the previous works so as to justify using the stochastic approach compared to the deterministic one.

This research was supported by the Brazilian institutions: Coordination for the Improvement of Higher Education Personnel (CAPES) - Finance Code 001, Brazilian National Council for Scientific and Technological Development (CNPq) under Grant 409359/2021-1, and the São Paulo Research Foundation (FAPESP), under grants 2015/21972-6, 2018/08008-4, 2022/03161-4, and Los Andes University. This article is a result of the project RETINA (NORTE-01-0145-FEDER-000062), supported by Norte Portugal Regional Operational Programme (NORTE 2020), under the PORTUGAL 2020 Partnership Agreement, through the European Regional Development Fund (ERDF). The authors acknowledge the work facilities and equipment provided by GECAD research center (UIDB/00760/2020) to the project team. João Soares also acknowledges FCT for grant CEECIND/00420/2022.

II. NOVELTY AND CONTRIBUTION

This paper proposes a novel nonlinear model for the coordinated operation of integrated gas and MG networks. The nonlinear formulation is sequentially linearized to guarantee the solution's optimality and decrease the computational burden. Finally, the deterministic linear model is transformed into a stochastic one to include uncertainties, and VSS is calculated to justify using the stochastic method adequately. Hence, the major contribution of this study can be summarized as:

- A novel nonlinear optimization model for the coordinated optimal operation of integrated natural gas distribution and MG networks
- Extracting mixed-integer linear programming (MILP) model via proper linearization to assure the optimality of the solutions
- Developing a scenario-based stochastic model to include uncertainties, while the value of the stochastic solution is embraced to justify stochastic model utilization

III. UNCERTAINTY MODELING AND SCENARIO GENERATION

This section presents the proper probability functions for modeling uncertainties linked to solar irradiation, wind speed, and energy demands. Also, it is explained how these probability density functions (PDFs) can be used to generate

7 scenarios. Moreover, the output power of PV and WT units according to solar irradiation and wind speed is modeled.

A. Wind Turbine and Weibull PDF

In the literature, Weibull PDF is used widely for modeling uncertainty related to wind speed. The Weibull PDF for variable x is presented in (1), in which k and c are shape and scale indices, and they can be calculated based on (2), where σ and μ denote standard deviation and expected value [8]. Moreover, the relationship between wind speed (V^{WT}) and the generated power by WT units (P^{WT}) can be presented as (3), in which V_{co}^{WT}, V_{ci}^{WT}, V_{no}^{WT}, and P_{no}^{WT} are cut-out speed, cut-in speed, nominal speed, and nominal capacity of the WT unit, respectively [8].

$$PDF(x) = e^{-\left(\frac{x}{c}\right)^k} \frac{k}{c}\left(\frac{x}{c}\right)^{k-1} \tag{1}$$

$$k = \left(\frac{\sigma}{\mu}\right)^{-1.086} \; \& \; c = \frac{\mu}{\Gamma\left(1+\frac{1}{k}\right)} \tag{2}$$

$$P^{WT} = \begin{cases} 0 \quad if \; V_{co}^{WT} < V^{WT} \; or \; V^{WT} < V_{ci}^{WT} \\ P_{no}^{WT}\left(\frac{V^{WT} - V_{ci}^{WT}}{V_{no}^{WT} - V_{ci}^{WT}}\right) \; if \; V_{ci}^{WT} < V^{WT} \leq V_{no}^{WT} \\ P_{no}^{WT} \quad if \; V_{no}^{WT} < V^{WT} \leq V_{co}^{WT} \end{cases} \tag{3}$$

B. Photovoltaic Unit and Beta PDF

The Beta PDF can be utilized to model the solar irradiance distribution [8]. The Beta PDF is presented in (4), where α and β (i.e., shape parameters) can be calculated according to (5). Furthermore, the relationship between the output power of PV units and solar irradiation is presented in (6), in which η^{PV} , S^{PV} , Φ^{PV} , and T^{O} are associated with conversion coefficient of PV unit, array area of PV unit, solar irradiance, and outdoor temperature [8].

$$PDF(x) = \frac{\Gamma(\alpha+\beta)}{\Gamma(\alpha)\Gamma(\beta)} x^{\alpha-1}(1-x)^{\beta-1} \tag{4}$$

$$\beta = (1-\mu)\left(\frac{\mu(1-\mu)}{\sigma^2} - 1\right) \; \& \; \alpha = \frac{\mu\beta}{1-\mu} \tag{5}$$

$$P^{PV} = \eta^{PV} S^{PV} \Phi^{PV}\left(1 - 0.005(T^{O} - 25)\right) \tag{6}$$

C. Electric Load, Gas demand, and Guassian PDF

Including uncertainties corresponding to electric load and gas demand is straightforward and Gaussian PDF is commonly used for this purpose [8], which is presented in (7).

$$PDF(x) = \frac{1}{\sigma\sqrt{2\pi}} e^{-\frac{(x-\mu)^2}{2\sigma^2}} \tag{7}$$

D. Scenario Generation

The aforementioned PDFs can be used for scenario generation to create the stochastic programming model. In this paper, the PDF of each uncertain parameter (x) is estimated by considering a few number of intervals [9]. The probability of each scenario (n_x) is obtained according to (8), where ρ_{x,n_x} corresponds with the respective probability [8], [9]. It is noteworthy that similar to references [8] and [9], the number of scenarios are considered 7 in this paper and the intervals are considered based on deviation in the forecasted values (i.e.,$-3\sigma, -2\sigma, -\sigma, 0, \sigma, 2\sigma, 3\sigma$).

$$\rho_{x,n_x} = \int_{x_{start}}^{x_{end}} xPDF(x)dx \tag{8}$$

IV. Mathematical Formulation

In this section, firstly, a mixed-integer nonlinear programming model for the optimal coordinated operation of gas and MG networks are presented. Then, the model is linearized, and MILP model is extracted. It is noteworthy that in the deterministic approach, it is assumed that all the parameters are crisp numbers and uncertainty is neglected. Finally, the respective MILP model is extended by considering different scenarios for uncertain parameters and the two-stage scenario-based stochastic model is created.

A. Deterministic Model

The objective function of this model is presented in (9) including cost minimization for both natural gas distribution network and MG. First term models the cost related to energy which is exchanged between MG and the main grid, where Ψ_t^{GR} is the electricity price and P_t^{GR} is the power exchanged between the MG and the main grid, and Δ_t corresponds to time interval. The second term is associated with quadratic cost of power generated by DG units, in which Ψ_{dg}^{a}, Ψ_{dg}^{b}, and Ψ_{dg}^{c} are cost coefficients. $\vartheta_{dg,t}^{DG}$ is the binary variable to indicate the commitment of DG units and $P_{dg,t}^{DG}$ is related to power generation of DG units. The third term is involved to model the cost of load shedding, where $P_{m,t}^{D}$, $\psi_{m,t}^{SHED}$, and $\Psi^{SHED}$are electric load demand, the proportion of load that is shed, and cost of load shedding. The last term is related to cost of natural gas distribution network, in which Ψ^{GAS}, $F_{g,t}^{S}$, and $F_{g,t}^{DG}$ are associated with price of natural gas, flow of inserted gas in the gas network, and the amount of gas exported to MG to be used by gas-fired DG units. Constraints (10)–(13) are embraced to model steady state power flow in MG. Constraints (10) and (11) ensure the active and reactive power balances in the MG, where $P_{km,t}$, $P_{pv,t}^{PV}$, $P_{wt,t}^{WT}$, and $P_{bs,t}^{BS}$ are active power flowing in line km (from bus k to bus m), power generated by PV units, power generated by WT units, and power of batteries (charging/discharging). Similarly, $Q_{km,t}$, Q_t^{GR} , $Q_{dg,t}^{DG}$, and $Q_{m,t}^{D}$ are associated with reactive power flowing from bus k to bus m, reactive power exchanged between the main grid and the MG, reactive power generated by DG units, and reactive power demand. Parameters R_{mn} and X_{mn} correspond to resistance and reactance of line mn. In addition, $I_{mn,t}^{sqr}$ is associated with square of current flowing in line mn. Constraint (12) shows the relationship between voltage of buses and active power, reactive power, and current flowing in lines of the MG. $V_{m,t}^{sqr}$and Z_{mn} are the square of voltage magnitude at bus m and impedance of line mn. The relationship between the current and active power, reactive power, and voltage of buses are included via constraint (13). The physical limitation linked to voltages and currents in MG is modeled via constraints (14) and (15), where $\overline{V}$ (upper bound of voltage), $\underline{V}$ (lower bound of voltage), and $\overline{I}$ (upper bound of current) are used to indicate the acceptable range of voltages and currents. Technical restrictions linked to DG units are considered via (16)–(19), in which $\underline{P}_{dg}^{DG}$ and $\overline{P}_{dg}^{DG}$ are lower and upper bounds for power generated by DG units and φ_{dg}^{DG} denotes power factor of DG units. Constraints related to operation of batteries are presented in (20)–(26), where $P_{bs,t}^{BS+}$ and $P_{bs,t}^{BS-}$ are nonnegative variables to model charging and discharging power of batteries. In addition, $\varrho_{bs,t}^{+}$ and $\varrho_{bs,t}^{-}$ are binary variables defined to avoid concurrent charging and discharging as considered in (23). Moreover, $\check{E}_{bs}^{BS}$, $E_{bs,t}^{BS}$, η_{bs}^{BS}, β_{bs}^{BS}, $\underline{E}^{BS}$, and $\overline{E}^{BS}$ are associated with initial energy, energy stored, efficiency, self-discharge rate, and minimum and maximum capacity of batteries. The low-pressure distribution gas network is modeled via constraints (27)–(31). In (27), the relationship between gas pressure and gas flow in low-pressure gas network (i.e., less than 75 mbar) is presented, which is known as Lacey's equation [10], where variables $\pi_{g,t}^{GAS}$ and $F_{gh,t}$ are the gas pressure at node g and gas flow from node g to node h in gas pipeline gh. In addition, parameters f, S^{GAS}, L^{PL}, and D^{PL} are associated with friction factor, specific gravity, length of pipeline, and diameter of pipeline. In (28), the natural gas flow balance is considered, where $F_{g,t}^{D}$ is the gas demand and in (29), the relationship between the natural gas and power generated by respective gas-fired DG units is modeled, in which Θ^{DG} corresponds to gas-to-power coefficient. Furthermore, the physical limits linked to pressure and gas flow are embraced in (30) and (31), where $\underline{\pi}^{GAS}$, $\overline{\pi}^{GAS}$, $\underline{F}_{gh}^{GAS}$, and $\overline{F}_{gh}^{GAS}$ denote the lower and upper bounds for gas pressure at nodes and gas flowing in pipeline gh. In (9)–(31), a deterministic and nonlinear model for coordinated optimal operation of integrated natural gas and MG networks is presented. To approximate the nonlinear model by an MILP model, the objective function and constraints (13) and (27) must be linearized via piecewise linearization approach [11]. In (32), the linearized objective function is presented, where ${P_{dg,t}^{DG}}^2$ is approximated by the product of slope ($m_{dg,\omega}^{DG}$) and discretization variable ($\Delta P_{dg,t,\omega}^{DG}$) for DG generation. The rest of limits related to linearization of ${P_{dg,t}^{DG}}^2$ are presented in (33) and (34), in which $\overline{\Delta P}_{dg}^{DG}$ and $m_{dg,\omega}^{DG}$ can be calculated according to equations (35) and (36), where $\overline{\omega}$ is the number of pieces. Similarly, constraints (13) and (27) are replaced by (37) and (38), respectively [11]. In addition, constraints (39)–(47) must be added to complete the linearization of the objective function. In a similar way, variables $P_{mn,t}^2$ and $Q_{mn,t}^2$ are approximated by the product of $m_{mn,\omega}^{PQ}$ (slope) and $\Delta P_{mn,t,\omega}$ (discrete block of active power) and $\Delta Q_{mn,t,\omega}$ (discrete block of reactive power). Parameters $V_{n,t}^{est}$, $m_{mn,\omega}^{PQ}$, and $\Delta Q_{mn,t,\omega}$ can be calculated according to (48)–(50). Similarly, $F_{gh,t}^2$ is linearized, the value of parameters $\overline{\Delta F}_{gh}$ and $m_{gh,\omega}^{PQ}$ are calculated via (51) and (52).

$$\min(obj) = \Bigg(\sum_t \Delta_t \Psi_t^{GR} P_t^{GR} + \Bigg(\sum_{dg}\sum_t \Psi_{dg}^{a}\vartheta_{dg,t}^{DG} + \Delta_t P_{dg,t}^{DG}\Psi^{b} + {P_{dg,t}^{DG}}^2 \Psi^{c}\Bigg) + \sum_m \sum_t \Delta_t P_{m,t}^{D}\,\psi_{m,t}^{SHED}\,\Psi^{SHED}\Bigg) + \Bigg(\sum_g\sum_t \Psi^{GAS}\big(F_{g,t}^{S} - F_{g,t}^{DG}\big)\Bigg) \tag{9}$$

$$\sum_{km} P_{km,t} - \sum_{mn}\big(P_{mn,t} + R_{mn} I_{mn,t}^{sqr}\big) + P_t^{GR} + \sum_{dg|b_{dg}=m} P_{dg,t}^{DG} + \sum_{pv|b_{pv}=m} P_{pv,t}^{PV} + \sum_{wt|b_{wt}=m} P_{wt,t}^{WT} = P_{m,t}^{D}\big(1-\psi_{n,t}^{SHED}\big) + \sum_{bs|b_{bs}=m} P_{bs,t}^{BS}\,; \forall m,t \tag{10}$$

$$\sum_{km} Q_{km,t} - \sum_{mn}\big(Q_{mn,t} + X_{mn} I_{mn,t}^{sqr}\big) + Q_t^{GR} + \sum_{dg|b_{dg}=m} Q_{dg,t}^{DG} = Q_{m,t}^{D};\ \forall m,t \tag{11}$$

$$V_{m,t}^{sqr} - V_{n,t}^{sqr} = 2\big(R_{mn}P_{mn,t} + X_{mn}Q_{mn,t}\big) + Z_{mn}^2 I_{mn,t}^{sqr};\ \forall mn,t \tag{12}$$

$$V_{n,t}^{sqr} I_{mn,t}^{sqr} = \big(P_{mn,t}^2 + Q_{mn,t}^2\big);\ \forall mn,t \tag{13}$$

$$\underline{V}^2 \le V_{n,t}^{sqr} \le \overline{V}^2;\ \forall n,t \tag{14}$$

$$0 \le I_{mn,t}^{sqr} \le \overline{I}^2;\ \forall mn,t \tag{15}$$

$$P_{dg,t}^{DG} \ge \vartheta_{dg,t}^{DG}\underline{P}_{dg}^{DG};\ \forall dg,t \tag{16}$$

$$P_{dg,t}^{DG} \le \vartheta_{dg,t}^{DG}\overline{P}_{dg}^{DG};\ \forall dg,t \tag{17}$$

$$Q_{dg,t}^{DG} \le P_{dg,t}^{DG}\tan\big(\cos^{-1}(\varphi_{dg}^{DG})\big);\ \forall dg,t \tag{18}$$

$$Q_{dg,t}^{DG} \ge -P_{dg,t}^{DG}\tan\big(\cos^{-1}(\varphi_{dg}^{DG})\big);\ \forall dg,t \tag{19}$$

$$0 \le P_{bs,t}^{BS+} \le \overline{P}_{bs}^{BS}\varrho_{bs,t}^{+};\ \forall bs,t \tag{20}$$

$$0 \le P_{bs,t}^{BS-} \le \overline{P}_{bs}^{BS}\varrho_{bs,t}^{-};\ \forall bs,t \tag{21}$$

$$P_{bs,t}^{BS} = P_{bs,t}^{BS+} - P_{bs,t}^{BS-};\ \forall bs,t \tag{22}$$

$$\varrho_{bs,t}^{+} + \varrho_{bs,t}^{-} \le 1;\ \forall bs,t \tag{23}$$

$$E_{bs,t}^{BS} = \check{E}_{bs}^{BS} + \Delta t\left(P_{bs,t}^{BS+}\eta_{bs}^{BS} - \frac{P_{bs,t}^{BS-}}{\eta_{bs}^{BS}} - E_{bs,t}^{BS}\beta_{bs}^{BS}\right);\ \forall bs,t|t = 1 \tag{24}$$

$$E_{bs,t}^{BS} = E_{bs,t-1}^{BS} + \Delta t\left(P_{bs,t}^{BS+}\eta_{bs}^{BS} - \frac{P_{bs,t}^{BS-}}{\eta_{bs}^{BS}} - E_{bs,t}^{BS}\beta_{bs}^{BS}\right);\quad \forall bs,t|t \ge 1 \tag{25}$$

$$\underline{E}^{BS} \le E_{bs,t}^{BS} \le \overline{E}^{BS};\ \forall bs,t \tag{26}$$

$$\pi_{g,t}^{GAS} - \pi_{h,t}^{GAS} = \frac{10^8 f S^{GAS} L^{PL} F_{gh,t}^2}{5.72^2 (D^{PL})^5};\ \forall gh,t \tag{27}$$

$$\sum_{gh\in\Omega_{PL}} F_{gh,t} + F_{g,t}^{D} + F_{g,t}^{DG} = F_{g,t}^{S};\ \forall g,t \tag{28}$$

$$P_{dg,t}^{DG} = F_{g,t}^{DG}\Theta^{DG};\forall t \tag{29}$$

$$\underline{\pi}^{GAS} \le \pi_{g,t}^{GAS} \le \overline{\pi}^{GAS};\ \forall g,t \tag{30}$$

$$\underline{F}_{gh}^{GAS} \le F_{gh,t} \le \overline{F}_{gh}^{GAS};\ \forall gh,t \tag{31}$$

$$\min(obj) = \Bigg(\sum_t \Delta_t \Psi_t^{GR} P_t^{GR} + \Bigg(\sum_{dg}\sum_t \Psi_{dg}^{a}\vartheta_{dg,t}^{DG} + \Delta_t P_{dg,t}^{DG}\Psi_{dg}^{b} + \sum_{\omega}\big(m_{dg,\omega}^{DG}\Delta P_{dg,t,\omega}^{DG}\big)\Psi_{dg}^{c}\Bigg) + \sum_m \sum_t \Delta_t P_{m,t}^{D}\,\psi_{m,t}^{SHED}\,\Psi^{SHED}\Bigg) + \Bigg(\sum_g\sum_t \Psi^{GAS}\big(F_{g,t}^{S} - F_{g,t}^{DG}\big)\Bigg) \tag{32}$$

$$P_{dg,t}^{DG} = \sum_{\omega}\Delta P_{dg,t,\omega}^{DG} + \vartheta_{dg,t}^{DG}\underline{P}^{DG};\forall dg,t \tag{33}$$

$$\Delta P_{dg,t,\omega}^{DG} \le \overline{\Delta P}_{dg}^{DG};\ \forall dg,t,\omega \tag{34}$$

$$\overline{\Delta P}_{dg}^{DG} = \big(\overline{P}_{dg}^{DG} - \underline{P}_{dg}^{DG}\big)/\overline{\omega};\ \forall dg \tag{35}$$

$$m_{dg,\omega}^{DG} = (2\omega - 1)\overline{\Delta P}_{dg}^{DG};\forall dg,\omega \tag{36}$$

$$V_{n,t}^{est} I_{mn,t}^{sqr} = \sum_{\omega} m_{mn,\omega}^{PQ} \left(\Delta P_{mn,t,\omega} + \Delta Q_{mn,t,\omega} \right); \forall mn, t \tag{37}$$

$$\pi_{g,t}^{GAS} - \pi_{h,t}^{GAS} = \frac{10^8 f S^{GAS} L^{PL} \sum_{\omega} \left(m_{gh,\omega}^{F} \Delta F_{gh,t} \right)}{5.72^2 (D^{PL})^5}; \ \forall gh, t \tag{38}$$

$$P_{mn,t} = P_{mn,t}^{+} - P_{mn,t}^{-}; \ \forall mn, t \tag{39}$$

$$Q_{mn,t} = Q_{mn,t}^{+} - Q_{mn,t}^{-}; \ \forall mn, t \tag{40}$$

$$\sum_{\omega} \left(\Delta P_{mn,t,\omega} \right) = P_{mn,t}^{+} + P_{mn,t}^{-}; \ \forall mn, t \tag{41}$$

$$\sum_{\omega} \left(\Delta Q_{mn,t,\omega} \right) = Q_{mn,t}^{+} + Q_{mn,t}^{-}; \ \forall mn, t \tag{42}$$

$$\Delta P_{mn,t,\omega} \leq \overline{\Delta S}_{mn}; \ \forall mn, t, \omega \tag{43}$$

$$\Delta Q_{mn,t,\omega} \leq \overline{\Delta S}_{mn}; \ \forall mn, t, \omega \tag{44}$$

$$F_{gh,t} = F_{gh,t}^{+} - F_{gh,t}^{-}; \ \forall gh, t \tag{45}$$

$$\sum_{\omega} \left(\Delta F_{gh,t,\omega} \right) = F_{gh,t}^{+} + F_{gh,t}^{-}; \ \forall gh, t \tag{46}$$

$$\Delta F_{gh,t,\omega} \leq \overline{\Delta F}_{gh}; \ \forall gh, t, \omega \tag{47}$$

$$V_{n,t}^{est} = \left(\overline{V}^2 + \underline{V}^2 \right) / 2; \ \forall n, t \tag{48}$$

$$\overline{\Delta S}_{mn} = \left(\overline{VI}_{mn} \right) / \overline{\omega}; \ \forall mn \tag{49}$$

$$m_{mn,\omega}^{PQ} = (2\omega - 1) \overline{\Delta S}_{mn}; \ \forall mn, \omega \tag{50}$$

$$\overline{\Delta F}_{gh} = \left(\overline{F}_{gh}^{GAS} - \underline{F}_{gh}^{GAS} \right) / \overline{\omega}; \ \forall gh \tag{51}$$

$$m_{gh,\omega}^{PQ} = (2\omega - 1) \overline{\Delta F}_{gh}; \ \forall gh, \omega \tag{52}$$

B. Stochastic Model

The stochastic model is presented in (53)–(86). It is worth noting that commitment of DG units are considered the first stage (here-&-now) decisions, while the charging and discharging of batteries, generation of DG units, power exchanged between the main grid and MG, and natural gas injection gas injection are selected as the second stage (wait-&-see) variables.

$$\begin{aligned} \min(obj) = \sum_{dg} \sum_{t} \Psi_{dg}^{a} \vartheta_{dg,t}^{DG} + \sum_{s} \Pi_{s} \Bigg(\sum_{t} \Delta_t \Psi_{t,s}^{GR} P_{t,s}^{GR} \\ + \Bigg(\sum_{dg} \sum_{t} \Delta_t P_{dg,t,s}^{DG} \Psi_{dg}^{b} \\ + \sum_{\omega} \left(m_{dg,\omega}^{DG} \Delta P_{dg,t,\omega,s}^{DG} \right) \Psi_{dg}^{c} \Bigg) \\ + \sum_{m} \sum_{t} \Delta_t P_{m,t,s}^{D} \psi_{m,t,s}^{SHED} \Psi^{SHED} \Bigg) \\ + \Bigg(\sum_{g} \sum_{t} \Psi^{GAS} \left(F_{g,t,s}^{S} - F_{g,t,s}^{DG} \right) \Bigg) \end{aligned} \tag{53}$$

$$\begin{aligned} \sum_{km} P_{km,t,s} - \sum_{mn} \left(P_{mn,t,s} + R_{mn} I_{mn,t,s}^{sqr} \right) + P_{t,s}^{GR} \\ + \sum_{dg|b_{dg}=m} P_{dg,t,s}^{DG} + \sum_{pv|b_{pv}=m} P_{pv,t,s}^{PV} \\ + \sum_{wt|b_{wt}=m} P_{wt,t,s}^{WT} \\ = P_{m,t,s}^{D} \left(1 - \psi_{n,t,s}^{SHED} \right) \\ + \sum_{bs|b_{bs}=m} P_{bs,t,s}^{BS}; \ \forall m, t, s \end{aligned} \tag{54}$$

$$\begin{aligned} \sum_{km} Q_{km,t,s} - \sum_{mn} \left(Q_{mn,t,s} + X_{mn} I_{mn,t,s}^{sqr} \right) + Q_{t,s}^{GR} \\ + \sum_{dg|b_{dg}=m} Q_{dg,t,s}^{DG} = Q_{m,t,s}^{D}; \forall m, t, s \end{aligned} \tag{55}$$

$$\begin{aligned} V_{m,t,s}^{sqr} - V_{n,ts}^{sqr} = 2 \left(R_{mn} P_{mn,t,s} + X_{mn} Q_{mn,t,s} \right) \\ + Z_{mn}^{2} I_{mn,t,s}^{sqr}; \forall mn, t, s \end{aligned} \tag{56}$$

$$V_{n,t,s}^{est} I_{mn,t,s}^{sqr} = \sum_{\omega} m_{mn,\omega}^{PQ} \left(\Delta P_{mn,t,\omega} + \Delta Q_{mn,t,\omega} \right); \forall mn, t, s \tag{57}$$

$$\underline{V}^2 \leq V_{n,t,s}^{sqr} \leq \overline{V}^2; \ \forall m, t, s \tag{58}$$

$$0 \leq I_{mn,t,s}^{sqr} \leq \overline{I}^2; \ \forall mn, t, s \tag{59}$$

$$P_{dg,t,s}^{DG} \geq \vartheta_{dg,t}^{DG} \underline{P}_{dg}^{DG}; \ \forall dg, t, s \tag{60}$$

$$P_{dg,t,s}^{DG} \leq \vartheta_{dg,t}^{DG} \overline{P}_{dg}^{DG}; \forall dg, t, s \tag{61}$$

$$Q_{dg,t,s}^{DG} \leq P_{dg,t,s}^{DG} \tan\left(\cos^{-1}\left(\varphi_{dg}^{DG} \right) \right); \ \forall dg, t, s \tag{62}$$

$$Q_{dg,t,s}^{DG} \geq -P_{dg,t,s}^{DG} \tan\left(\cos^{-1}\left(\varphi_{dg}^{DG} \right) \right); \forall dg, t, s \tag{63}$$

$$0 \leq P_{bs,t,s}^{BS+} \leq \overline{P}_{bs}^{BS} \varrho_{bs,t,s}^{+}; \ \forall bs, t, s \tag{64}$$

$$0 \leq P_{bs,t,s}^{BS-} \leq \overline{P}_{bs}^{BS} \varrho_{bs,t,s}^{-}; \ \forall bs, t, s \tag{65}$$

$$P_{bs,t,s}^{BS} = P_{bs,t,s}^{BS+} - P_{bs,t,s}^{BS-}; \ \forall bs, t, s \tag{66}$$

$$\varrho_{bs,t,s}^{+} + \varrho_{bs,t,s}^{-} \leq 1; \ \forall bs, t, s \tag{67}$$

$$\begin{aligned} E_{bs,t,s}^{BS} = \check{E}_{bs}^{BS} + \Delta t \Bigg(P_{bs,t,s}^{BS+} \eta_{bs}^{BS} - \frac{P_{bs,t,s}^{BS-}}{\eta_{bs}^{BS}} \\ - E_{bs,t,s}^{BS} \beta_{bs}^{BS} \Bigg); \ \forall bs, t, s | t = 1 \end{aligned} \tag{68}$$

$$\begin{aligned} E_{bs,t,s}^{BS} = E_{bs,t-1,s}^{BS} + \Delta t \Bigg(P_{bs,t,s}^{BS+} \eta_{bs}^{BS} - \frac{P_{bs,t,s}^{BS-}}{\eta_{bs}^{BS}} \\ - E_{bs,t,s}^{BS} \beta_{bs}^{BS} \Bigg); \ \forall bs, t, s | t \geq 1 \end{aligned} \tag{69}$$

$$\underline{E}^{BS} \leq E_{bs,t,s}^{BS} \leq \overline{E}^{BS}; \ \forall bs, t, s \tag{70}$$

$$\pi_{g,t,s}^{GAS} - \pi_{h,t,s}^{GAS} = \frac{10^8 f S^{GAS} L^{PL} \sum_{\omega} \left(m_{gh,\omega}^{F} \Delta F_{gh,t,s} \right)}{5.72^2 (D^{PL})^5}; \forall gh, t, s \tag{71}$$

$$\sum_{gh} F_{gh,t,s} + F_{g,t,s}^{D} + F_{g,t,s}^{DG} = F_{g,t,s}^{S}; \ \forall g, t, s \tag{72}$$

$$P_{dg,t,s}^{DG} = F_{g,t,s}^{DG} \Theta^{DG}; \ \forall t, s \tag{73}$$

$$\underline{\pi}^{GAS} \leq \pi_{g,t,s}^{GAS} \leq \overline{\pi}^{GAS}; \ \forall g, t, s \tag{74}$$

$$\underline{F}_{gh}^{GAS} \leq F_{gh,t,s} \leq \overline{F}_{gh}^{GAS}; \ \forall gh, t, s \tag{75}$$

$$P_{dg,t,s}^{DG} = \sum_{\omega} \Delta P_{dg,t,\omega,s}^{DG} + \vartheta_{dg,t}^{DG} \underline{P}^{DG}; \forall dg, t, s \tag{76}$$

$$\Delta P_{dg,t,\omega,s}^{DG} \leq \overline{\Delta P}_{dg}^{DG}; \ \forall dg, t, \omega, s \tag{77}$$

$$P_{mn,t,s} = P_{mn,t,s}^{+} - P_{mn,t,s}^{-}; \ \forall mn, t, s \tag{78}$$

$$Q_{mn,t,s} = Q_{mn,t,s}^{+} - Q_{mn,t,s}^{-}; \ \forall mn, t, s \tag{79}$$

$$\sum_{\omega} \left(\Delta P_{mn,t,\omega,s} \right) = P_{mn,t,s}^{+} + P_{mn,t,s}^{-}; \ \forall mn, t, s \tag{80}$$

$$\sum_{\omega} \left(\Delta Q_{mn,t,\omega,s} \right) = Q_{mn,t,s}^{+} + Q_{mn,t,s}^{-}; \ \forall mn, t, s \tag{81}$$

$$\Delta P_{mn,t,\omega,s} \leq \overline{\Delta S}_{mn}; \ \forall mn, t, \omega, s \tag{82}$$

$$\Delta Q_{mn,t,\omega,s} \leq \overline{\Delta S}_{mn}; \ \forall mn, t, \omega, s \tag{83}$$

$$F_{gh,t,s} = F_{gh,t,s}^{+} - F_{gh,t,s}^{-}; \ \forall gh, t, s \tag{84}$$

$$\sum_{\omega} \left(\Delta F_{gh,t,\omega,s} \right) = F_{gh,t,s}^{+} + F_{gh,t,s}^{-}; \ \forall gh, t, s \tag{85}$$

$$\Delta F_{gh,t,\omega,s} \leq \overline{\Delta F_{gh}};\ \forall gh,t,\omega,s \tag{86}$$

C. *Value of the stochastic solution*

The value of the sstochastic solution is measurement to economically evaluate the performance of stochastic optimization over the deterministic one. The VSS can be calculated according to (87), where Z^{S*} is the optimal value of stochastic problem. To calculate Z^{D*}, firstly a deterministic model based on average value of scenarios is solved and first stage solutions are obtained. Then, the two-stage problem is solved for each scenario separately, while fixing the first stage decision variables to the solution of the aforementioned deterministic model [7].

$$VSS = Z^{D*} - Z^{S*} \tag{87}$$

V. Test and Results

To evaluate the proposed deterministic and stochastic models for the coordinated optimal operation of gas and MG networks, a modified IEEE 33-bus test network along with 11-node distribution natural gas network forming an integrated system as shown in Fig. 1. Moreover, the scenarios for electric load, electricity price, solar irradiation, and wind speed are illustrated in Fig. 2–Fig. 5. The data on MG components is presented in Table I and Table II, the data associated with gas distribution network can be found in [10]. It is worth noting that AMPL and CPLEX were used for modeling and solving the optimization models [12], and the models are run on a system with an Intel i5-1135G7 processor and 16 GB RAM.

A. *Case I: Deterministic*

In this case study, a deterministic model for the coordinated operation of integrated gas and MG networks without considering uncertainties is solved. The costs of the gas network and MG are \$4790.4 and \$2848.62, respectively, meaning that the total cost of the integrated system is \$7639.02. The scheduling of DG units and batteries is visualized in Fig. 6, showing that DG unit 3 is committed for the whole day, while DG unit 1 and DG unit 2 are committed partially. The power exchanged between MG and the main grid is depicted in Fig. 7 (positive value for buying and negative value for selling), indicating that when the electricity price is lower, the MG buys the power from the grid, and when the price is higher MG tries to not buy from or even tries to sell the power to the main grid. As aforementioned, the scheduling of MG should not violate any technical constraints, including voltage limits. Thus, Fig. 8 is shown to verify that the voltage magnitudes among all the buses during the entire day stay in the acceptable range ($\pm 5\%$).

B. *Case II: Stochastic*

This subsection presents the results associated with the proposed stochastic programming model for the optimal coordinated operation of integrated gas and MG networks. At the same time, the uncertainties are included via scenarios. The cost of the gas network and MG are obtained at \$3398.85 and \$2878.18, so the total cost of the integrated system reaches \$6277.03, indicating a 17.82% reduction in the total cost of the system compared to the deterministic approach. Furthermore, as mentioned before, VSS measurement can be used to economically justify using stochastic programming compared to the deterministic approach. Hence, the VSS for this study is \$1274.2 ($Z^{D*} = 7551.3$), showing a 16.87% decrease. Albeit the generation of DG units and charging and discharging of batteries are considered second-stage decision variables and their values depend on realization of uncertainties, it is still possible to show the average value of scheduling of DGs and batteries as depicted in Fig. 9, indicating changes in scheduling specifically for DG unit 3. The power exchanged between MG and the main grid is presented in Fig. 10, including all the realizations. The range of voltage considering all the scenarios and buses is depicted in Fig. 11, showing that the voltage limitation is satisfied.

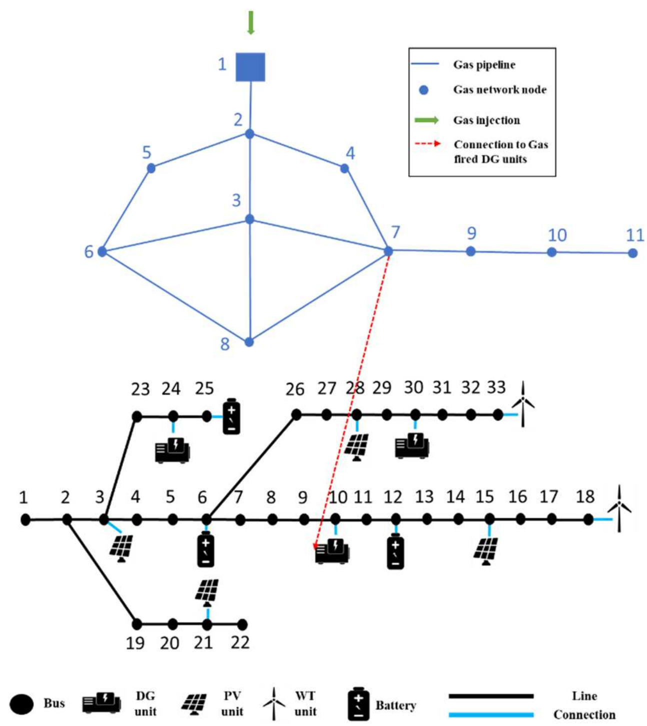

Fig. 1. Integrated gas distribution and MG networks

TABLE I. Data on Distributed Generation Units

Characteristic	DG unit 1	DG unit 2	DG unit 3
Bus	10	24	30
$\overline{P}_{dg}^{DG}$(kW)	900	1000	1500
$\underline{P}_{dg}^{DG}$(kW)	100	100	100
φ_{dg}	0.8	0.8	0.8
a_{dg}(\$)	27	25	26
b_{dg}(\$/MWh)	87	87	81
c_{dg}(\$/MWh^2)	0.0025	0.0035	0.184

TABLE II. Data on Batteries

Characteristic	Battery 1	Battery 2	Battery 3
Bus	6	12	25
$\overline{S}_{bs}^{BS}$(kW)	200	200	200
$\overline{E}_{bs}^{BS}$(kWh)	1200	900	900
$\underline{E}_{bs}^{BS}$(kWh)	200	150	150
η_{bs}^{Ch} & η_{bs}^{Dis}	0.95	0.94	0.96
β_{bs}	0.002	0.002	0.004

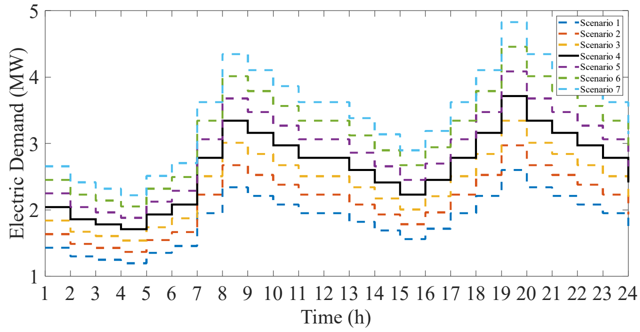

Fig. 2. Scenarios for electric demand

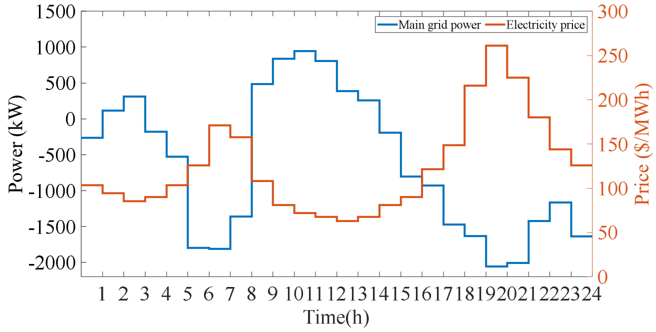

Fig. 7. Main grid power exchange in deterministic model

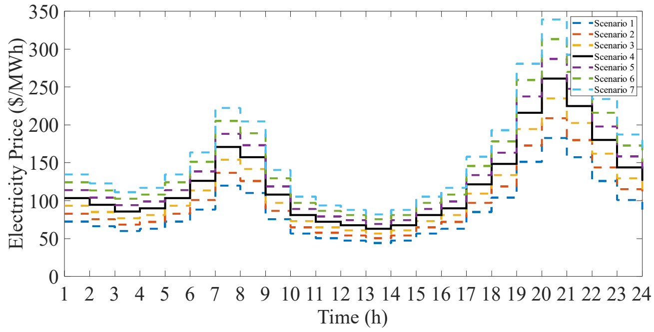

Fig. 3. Scenarios for Electricity price

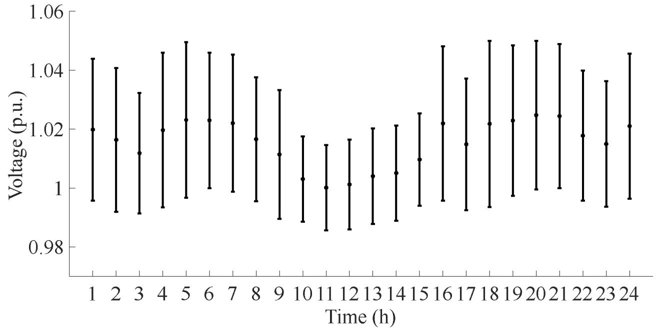

Fig. 8. Range of voltage magnitude in deterministic model

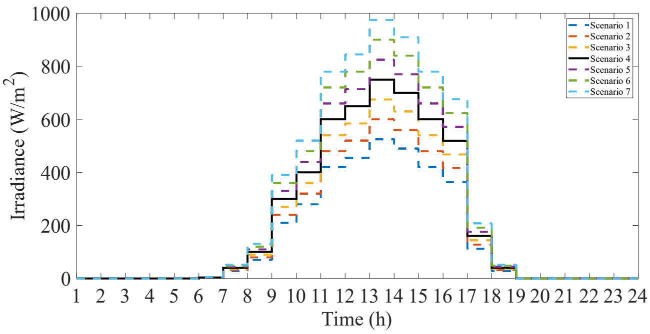

Fig. 4. Scenarios for solar irradiance

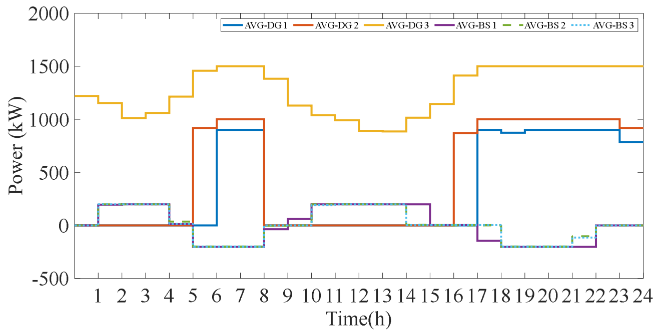

Fig. 9. Scheduling of DG units and batteries in stochastic model

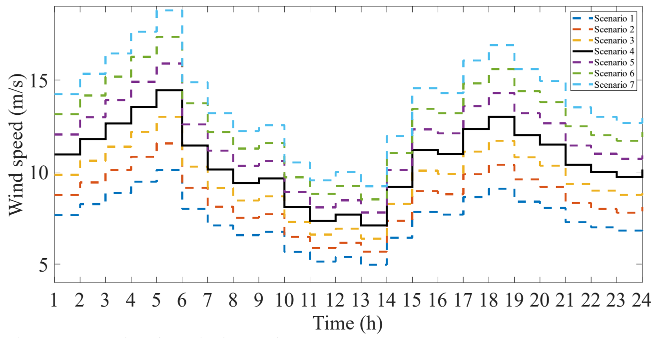

Fig. 5. Scenarios for wind speed

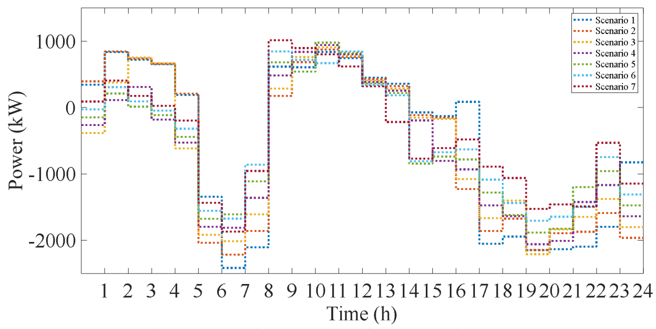

Fig. 10. Main grid power exchange in stochastic model

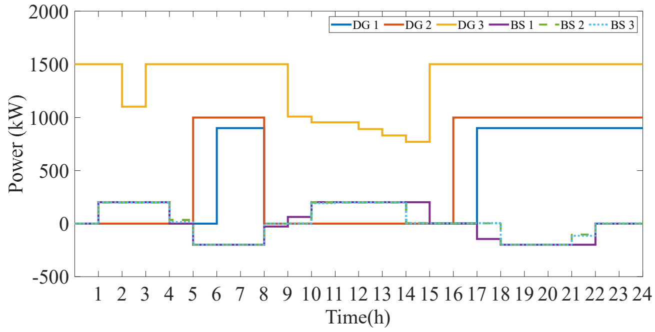

Fig. 6. Scheduling of DG units and batteries in deterministic model

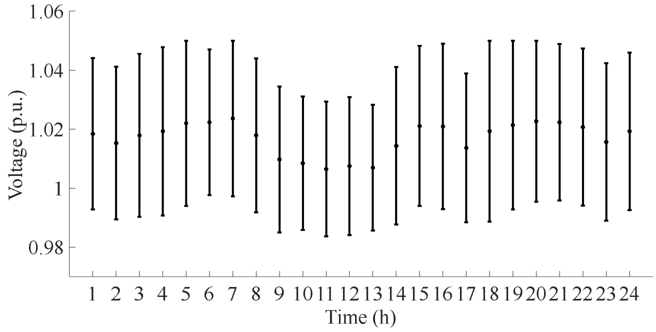

Fig. 11. Range of voltage magnitude in stochastic model

VI. CONCLUSION

Microgrids can effectively accommodate renewable energy-based distribution generation units such as wind power and photovoltaic units; nonetheless, the output of such generation units is intermittent and can adversely affect the energy management of microgrids. As a result, batteries and gas-fired dispatchable distributed generation can be used to cope with such fluctuations and mitigate their adverse effects on the operation of microgrids. Therefore, this paper proposed a mixed-integer linear programming model for the optimal coordinated operation of integrated natural gas distribution networks and microgrids. At the same time, photovoltaic and wind power units were included. In addition, uncertainties were considered via the scenario generation approach, and the value of stochastic solution measurement was obtained, showing the superiority of the stochastic model over the deterministic approach. The proposed model was tested on the integrated 11-node distribution network and a 33-bus microgrid. The results showed that the total cost of the integrated system decreased significantly in the stochastic model compared to the deterministic one.

REFERENCES

[1] S. Potrč, L. Čuček, M. Martin, and Z. Kravanja, "Sustainable renewable energy supply networks optimization–The gradual transition to a renewable energy system within the European Union by 2050," Renew. Sustain. Energy Rev., vol. 146, p. 111186, 2021.

[2] S. F. Zandrazavi, C. P. Guzman, A. T. Pozos, J. Quiros-Tortos, and J. F. Franco, "Stochastic multi-objective optimal energy management of grid-connected unbalanced microgrids with renewable energy generation and plug-in electric vehicles," Energy, vol. 241, p. 122884, 2022.

[3] J. Duan, Y. Yang, and F. Liu, "Distributed optimization of integrated electricity-natural gas distribution networks considering wind power uncertainties," Int. J. Electr. Power Energy Syst., vol. 135, p. 107460, 2022.

[4] Z. Wang et al., "Multi-stage stochastic programming for resilient integrated electricity and natural gas distribution systems against typhoon natural disaster attacks," Renew. Sustain. Energy Rev., vol. 159, p. 111784, 2022.

[5] V. Shabazbegian, H. Ameli, M. T. Ameli, G. Strbac, and M. Qadrdan, "Co-optimization of resilient gas and electricity networks; a novel possibilistic chance-constrained programming approach," Appl. Energy, vol. 284, p. 116284, 2021.

[6] V. Shabazbegian, H. Ameli, M. T. Ameli, and G. Strbac, "Stochastic optimization model for coordinated operation of natural gas and electricity networks," Comput. Chem. Eng., vol. 142, p. 107060, 2020.

[7] J. Soares, M. A. Fotouhi Ghazvini, N. Borges, and Z. Vale, "A stochastic model for energy resources management considering demand response in smart grids," Electr. Power Syst. Res., vol. 143, pp. 599–610, 2017.

[8] R. Bahmani, H. Karimi, and S. Jadid, "Stochastic electricity market model in networked microgrids considering demand response programs and renewable energy sources," Int. J. Electr. Power Energy Syst., vol. 117, p. 105606, 2020.

[9] H. Karimi and S. Jadid, "Optimal energy management for multi-microgrid considering demand response programs: A stochastic multi-objective framework," Energy, vol. 195, p. 116992, 2020.

[10] M. Abeysekera, J. Wu, N. Jenkins, and M. Rees, "Steady state analysis of gas networks with distributed injection of alternative gas," Appl. Energy, vol. 164, pp. 991–1002, 2016.

[11] T. D. De Lima, J. F. Franco, F. Lezama, and J. Soares, "A specialized long-term distribution system expansion planning method with the integration of distributed energy resources," IEEE Access, vol. 10, pp. 19133–19148, 2022.

[12] I. ILOG, "AMPL CPLEX System Version 11 User's Guide," ILOG CPLEX Div., 2008.